



Assessment of geocenter motion estimates from the IGS second reprocessing

Yifang Ma^{1,2,3,4} · Paul Rebischung^{2,3} · Zuheir Altamimi^{2,3} · Weiping Jiang¹

Received: 14 January 2019 / Accepted: 28 February 2020 / Published online: 10 March 2020
© Springer-Verlag GmbH Germany, part of Springer Nature 2020

Abstract

We investigate geocenter motion time series derived from the combined solutions and six individual analysis center (AC) solutions of the International GNSS Service (IGS) second reprocessing campaign using the network shift approach, in terms of noise content, long-term trends, periodic and aperiodic variations. We assess these GNSS geocenter motion estimates by comparison with independent estimates from satellite laser ranging (SLR). The GNSS geocenter time series exhibit correlated noise which is better represented by a white plus power-law noise model in the X and Y directions, and by a white plus first-order autoregressive (or generalized Gauss–Markov) noise model in the Z direction. The GNSS geocenter time series include expected seasonal variations, but also spurious draconitic signals, particularly in the Z direction. GNSS annual geocenter motion estimates are in reasonable agreement with SLR estimates in the X and Y directions. In the Z direction, however, the annual signals derived from the IGS solutions disagree with SLR estimates, except for three particular ACs. This suggests that the different orbit modeling strategies used by these ACs may constitute an improvement over the conventional strategy employed by the other ACs. The background noise in GNSS and SLR geocenter time series finally appears to be correlated, suggesting that it might partly reflect real, aperiodic geocenter motion.

Keywords GNSS · SLR · Geocenter motion · Network shift approach · IGS · ILRS

Introduction

Geocenter motion is defined as the relative motion between the center of mass (CM) of the total Earth system and the center of figure (CF) of the solid Earth surface (Dong et al. 1997; Ray 1999). As described by Wu et al. (2012), geocenter motion is caused by mass redistributions within the Earth system with multi-temporal variations, including sub-daily and daily periods, seasonal and interannual periods and long-term variations. The accurate measurement of geocenter motion is important for the determination of global and regional surface mass variability (Blewitt and

Clarke 2003; Wu et al. 2012). Geocenter motion is also fundamentally related to the definition and realization of the International Terrestrial Reference Frame (ITRF) origin so that a detailed investigation of geocenter motion derived from geodetic measurements is required for improving the realization of the ITRF origin (Blewitt 2003; Dong et al. 2003; Petit and Luzum 2010).

Two main methods exist for estimating geocenter motions from space geodetic observations. The first one consists in estimating the translational offset between CM and CF directly and is called “network shift approach” (Blewitt et al. 1992; Wu et al. 2012). The ITRF origin is determined from a long-term stacking of CM-centered frames and hence follows the long-term averaged CM. Over short and seasonal time scales, however, the ITRF origin approximately follows CF (Dong et al. 2003; Collilieux et al. 2009; Altamimi et al. 2016). On the other hand, the origin of Earth satellite orbits is CM according to the orbit dynamics theory. Station–satellite range measurements at given epochs can thus be processed to estimate station coordinates and satellite orbits simultaneously in theoretically CM-centered frames. Helmert transformation parameters can then be estimated

✉ Yifang Ma
yfangma@whu.edu.cn

¹ GNSS Research Center, Wuhan University, 129 Luoyu Road, Wuhan 430079, China

² Institut de physique du globe de Paris, CNRS, IGN, Université de Paris, 75005 Paris, France

³ ENSG-Géomatique, IGN, 77455 Marne-la-Vallée, France

⁴ Beijing Earthquake Agency, Beijing 100080, China

between such CM-centered frames and the ITRF, and the translational parameters obtained represent in principle geocenter motion at sub-secular time scales. In theory, SLR, Global Navigation Satellite System (GNSS) and Doppler Orbitography and Radiopositioning Integrated by Satellite (DORIS) solutions could be used to estimate geocenter motion by the network shift approach. However, only SLR geocenter estimates are currently considered and reliable enough to contribute to the definition of the ITRF origin. Although the GNSS tracking network and satellite constellation are superior to those of SLR, GNSS geocenter motion estimates obtained by the network shift approach exhibit larger errors than SLR results and do not contribute to the ITRF origin. Due to severe correlation (collinearity) with other parameters, geocenter coordinates are indeed weakly observable in GNSS analyses (Rebischung et al. 2014), hence prone to contamination by modeling errors. Several researches indicate that GNSS network shift results are in particular biased by orbit modeling errors (Dong et al. 2003; Rodriguez-Solano et al. 2012; Meindl et al. 2013).

The second method is an inverse method, called “degree-1 deformation approach” (Blewitt et al. 2001; Lavalette et al. 2006; Zhang and Jin 2014). It consists in estimating degree-1 surface mass load coefficients from the observed deformation of a globally distributed geodetic network, for instance, a GNSS tracking network, and converting the load coefficients into equivalent geocenter motion. The degree-1 deformation approach cannot sense secular geocenter motion and cannot contribute to the definition of the ITRF origin.

We focus on geocenter estimates obtained from recent GNSS solutions using the network shift approach. The second IGS (Johnston et al. 2017) reprocessing campaign (repro2; <https://acc.igs.org/reprocess2.html>) was finalized in 2015 by different ACs, and daily combinations of the AC solutions were provided as the IGS input to the latest ITRF solution (ITRF2014; Altamimi et al. 2016). The daily repro2 combined geocenter coordinates with respect to the IGB08 reference frame, whose origin inherits from ITRF2008, were analyzed by Rebischung et al. (2016). The results show that

the offsets and rates of the repro2 combined geocenter time series lie within the uncertainties of the origin and origin rate of ITRF2008 except a 7 mm offset in the Z component. The annual signals in the repro2 geocenter time series are in good agreement in phase with SLR results in the X and Y directions but are mostly out of phase in the Z direction. We extend those results by analyzing geocenter motion time series derived from six individual AC solutions and from the repro2 combined solutions, and by comparing them with SLR results.

This study has two purposes: First, by analyzing geocenter time series from different ACs, we wish to evaluate the impact of different analysis strategies on GNSS geocenter motion estimates and determine whether particular strategies lead to improved geocenter motion estimates. Second, by characterizing and modeling the time-correlated noise present in the GNSS geocenter motion time series, we wish to provide realistic uncertainties for the trends and seasonal signals inferred from those time series.

Data and methods

Geocenter coordinates with respect to the ITRF2014 origin were derived from the repro2 daily solutions of six ACs and from the IGS repro2 combined solutions, using the method described by Rebischung et al. (2016). The AC repro2 geocenter series were extended until GPS week 1831 (2015-02-14) based on daily operational solutions, as reported in Table 1 of Rebischung et al. (2016). The geocenter time series derived from the GRGS, ULR and GFZ-TIGA repro2 solutions were not considered as they either show large spurious behaviors (Rebischung et al. 2016) or would have been redundant with geocenter estimates derived from the (standard) GFZ repro2 solutions. Note that not all GNSS stations in ITRF2014 were used to define the reference frame of the daily AC solutions (i.e., for the application of no-net-rotation and no-net-translation constraints), but only the same subset of 252 stations with long and stable station position time

Table 1 Geocenter motion time series considered in this study

Name	Data span	Sampling	Data source
ig2	1994/01–2015/02	Daily	International GNSS Service; Rebischung et al. (2016)
cf2	1994/01–2015/02	Daily	Center for Orbit Determination in Europe; Steigenberger et al. (2014)
em2	1994/10–2015/02	Daily	Natural Resources Canada; Donahue et al. (2014)
es2	1995/01–2015/02	Daily	European Space Operations Center; Springer et al. (2014)
gf2	1994/01–2015/02	Daily	GeoForschungsZentrum; Deng et al. (2014)
jp2	1994/01–2015/02	Daily	Jet Propulsion Laboratory; Desai et al. (2014)
mi2	1994/01–2015/02	Daily	Massachusetts Institute of Technology
SLR	1994/01–2014/12	Weekly	Altamimi et al. (2016)
SLR–GRACE	2002/08–2014/12	Weekly	Altamimi et al. (2016); Lemoine et al. (2013)

series that were selected to define the IGS14 reference frame (Rebischung and Schmid, 2016). Besides, as described in Rebischung et al. (2016), an iterative screening of the residuals from a 6-parameter transformation between each daily AC solution and the restricted ITRF2014 was performed, in order to remove possible outliers from the set of reference frame defining stations.

We used two SLR geocenter motion sets for comparison. The first SLR geocenter estimates are the translations estimated by Altamimi et al. (2016) between the weekly SLR input solutions to ITRF2014 provided by the International Laser Ranging Service (ILRS; Pearlman et al. 2002) and ITRF2014. Such net translations are, however, known to provide imperfect geocenter estimates, owing to the “network effect,” i.e., the fact that the individual motions of the unevenly distributed SLR stations make the center of the SLR network move relatively to CF (Collilieux et al. 2009). Several recent studies have thus found the impact of this network effect on the amplitude of SLR-derived annual geocenter motion to be as large as about 3 mm in the Z direction and about 1 mm in the X direction (Ries 2016; Kang et al. 2019). We therefore introduce a second set of SLR-based geocenter estimates, in which the network effect is mitigated using GRACE-derived loading displacement time series of the SLR stations. Those loading displacement time series are derived from the Stokes coefficients of degrees 2–80 of the GRGS RL03-v3 10-day GRACE solutions (Lemoine et al. 2013) as described in Chanard et al. (2018). Note that all Stokes coefficient time series have been detrended and corrected for co- and post-seismic signals, so that the computed loading displacements are also trend-free. Those GRACE-derived loading displacements are then linearly interpolated to weekly intervals and removed from the weekly SLR input solutions to ITRF2014, and translations are finally estimated between the weekly loading-corrected SLR solutions and ITRF2014. These results are denoted hereafter as “SLR–GRACE.” Note that since we aim at evaluating the original geocenter time series derived from different IGS AC repro2 solutions, and since the network effect on GNSS geocenter estimates is relatively small (i.e., ≤ 0.5 mm on annual amplitudes, (Collilieux et al. 2012; Zou et al. 2014), we did not attempt to mitigate the network effect in the GNSS geocenter time series considered here.

Table 1 summarizes the nine geocenter time series compared in this study. Figures 1 and 2 show the nine geocenter coordinate time series and the square root of their power spectral densities (PSDs). The PSDs are obtained from Lomb–Scargle periodograms (Scargle 1982). The GNSS-derived geocenter time series appear more scattered than the SLR time series, especially before 2002. As geophysically expected, the PSDs of all the time series exhibit large peaks at the annual frequency. Small spectral peaks at the semi-annual frequency are discernible in some cases, mainly in

the X component. Spurious spectral peaks at harmonics of the GPS draconitic year, i.e., the period at which the orientation of the GPS constellation with respect to the Sun repeats (about 351.4 days/1.04 cpy; Ray et al. 2008), are additionally visible for GNSS-derived time series, and particularly pronounced at odd draconitic harmonics in the Z direction. The Z component of the cf2 time series shows a particularly large peak at the third draconitic harmonic, likely related to the use of GLONASS data (see Figure 2 in Meindl et al. 2013).

Based on their PSDs, we decided on the parametric models used to represent the different geocenter time series in our analysis. SLR-derived time series were thus represented by a linear trend, plus annual and semi-annual periodic terms, while our parametric models for GNSS-derived time series included additional periodic terms at the first eight draconitic harmonics. As for the stochastic variations in the time series, different noise models were tried and compared, namely a pure white noise model referred to as wh, a white plus power-law noise model referred to as wh + pl, a white plus flicker noise model referred to as wh + fl, a white plus generalized Gauss–Markov noise model referred to as wh + GGM and a white plus first-order autoregressive noise model referred to as wh + AR(1).

Results and discussion

This section analyzes the nine geocenter coordinate time series listed in Table 1. We establish the preferred noise models for all the geocenter time series and then investigate the long-term linear trends, apparent annual variations and aperiodic signals of those geocenter motion time series based on their preferred noise models.

Noise models

The noise content of GNSS station position time series has been extensively studied and found to be generally best described by a combination of white and flicker noise (Zhang et al. 1997; Mao et al. 1999; Williams et al. 2004; Amiri-Simkooei 2007, 2009; Santamaría-Gómez et al. 2011). However, the noise content of GNSS-derived geocenter time series has not been characterized yet. Characterizing the noise content of GNSS-derived geocenter estimates may help identify the noise sources and provide an indication for future noise reduction. Also, modeling the noise in GNSS-derived geocenter time series realistically is necessary to assess the significance of parameters, such as trends and periodic signals, derived from the time series.

To analyze the noise content of the geocenter time series shown in Fig. 1, we used the Hector software (Bos et al. 2013). We fitted the five considered noise models to all time series, simultaneously with the parametric models described

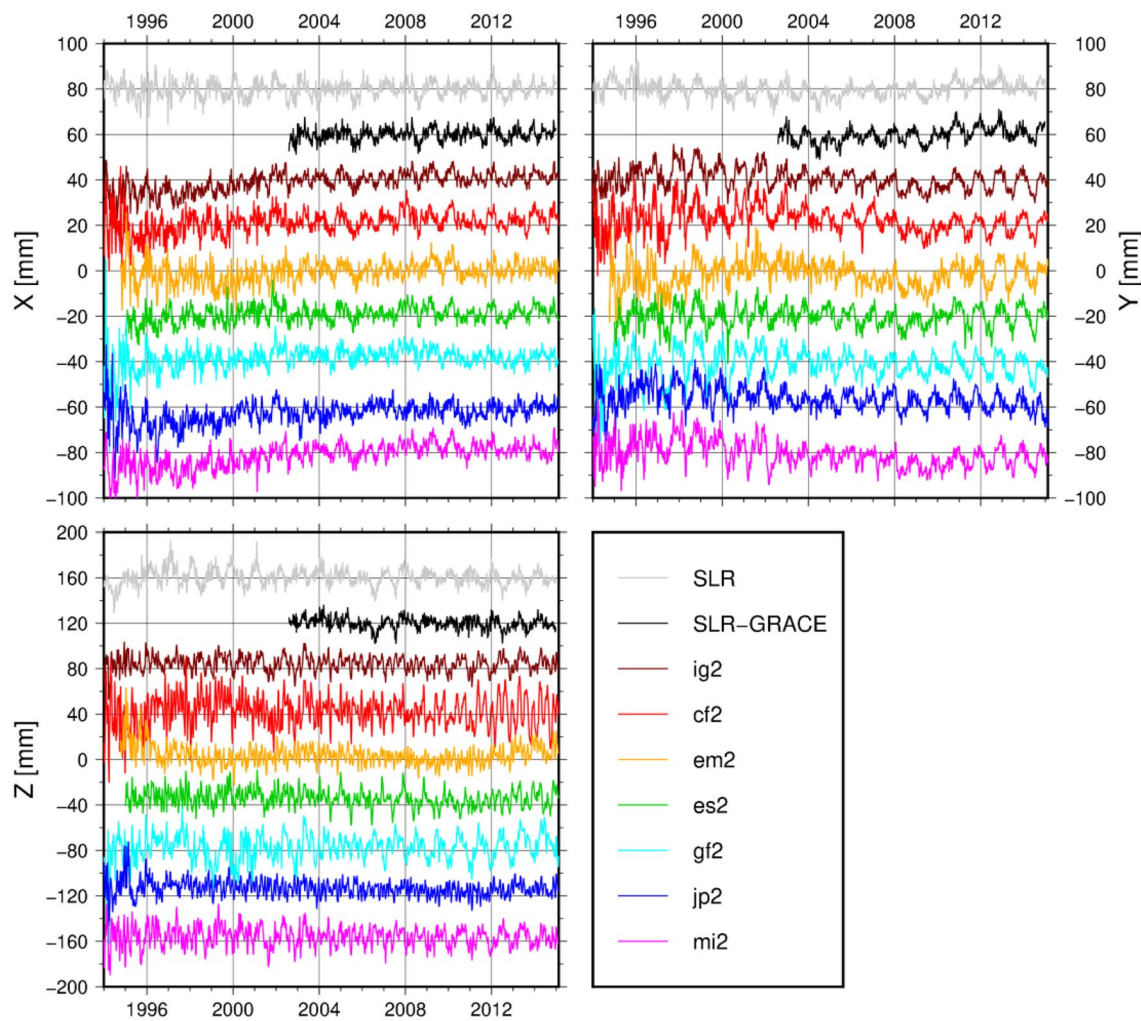


Fig. 1 Geocenter coordinate time series. Offsets of 20, 20 and 40 mm have been added for clarity in the X, Y and Z directions

above. The Bayesian information criterion (BIC; Schwarz 1978; values given in Table 2) was then used to identify a single preferred noise model for each time series. The preferred noise models (i.e., the ones with minimum BIC values) are listed in Table 3 with their parameters (i.e., the spectral indices of wh + fl, wh + pl and wh + GGM noise models, and the autoregression parameters φ of wh + AR(1) and wh + GGM models; see parameter definitions in Bos and Fernandes 2019).

Table 3 shows that all considered geocenter time series exhibit correlated noise, although of various natures. In the X direction, the noise in all GNSS time series is well fitted by wh + pl models, with spectral indices of about -0.7 . In the Y direction, wh + fl models are preferred for most GNSS time series. On the other hand, either wh + AR(1) or wh+GGM models better describe the noise in the Z component of the GNSS time series. As regards SLR-based time series, wh + AR(1) models are preferred

in the X component, while wh + fl models are preferred in the Y and Z components. The PSDs of the residual geocenter time series are in good accordance with those of the corresponding preferred noise models, as shown in Fig. 3, indicating the suitability of the models. It should be noted that all results presented in the next sections are based on those preferred noise models.

Although periodic terms at the first eight draconitic harmonics have been included in our parametric model for GNSS time series, spectral peaks around some draconitic harmonics are still discernible in the PSDs of the GNSS residual time series in Fig. 3, similarly as in Figure 8 of Amiri-Simkooei et al. (2017). This indicates that the draconitic variations in the GNSS geocenter series are not completely stationary with time. Most of the draconitic variations have nevertheless been captured by the estimated periodic terms, and the remaining spectral peaks are relatively small compared to the background noise.

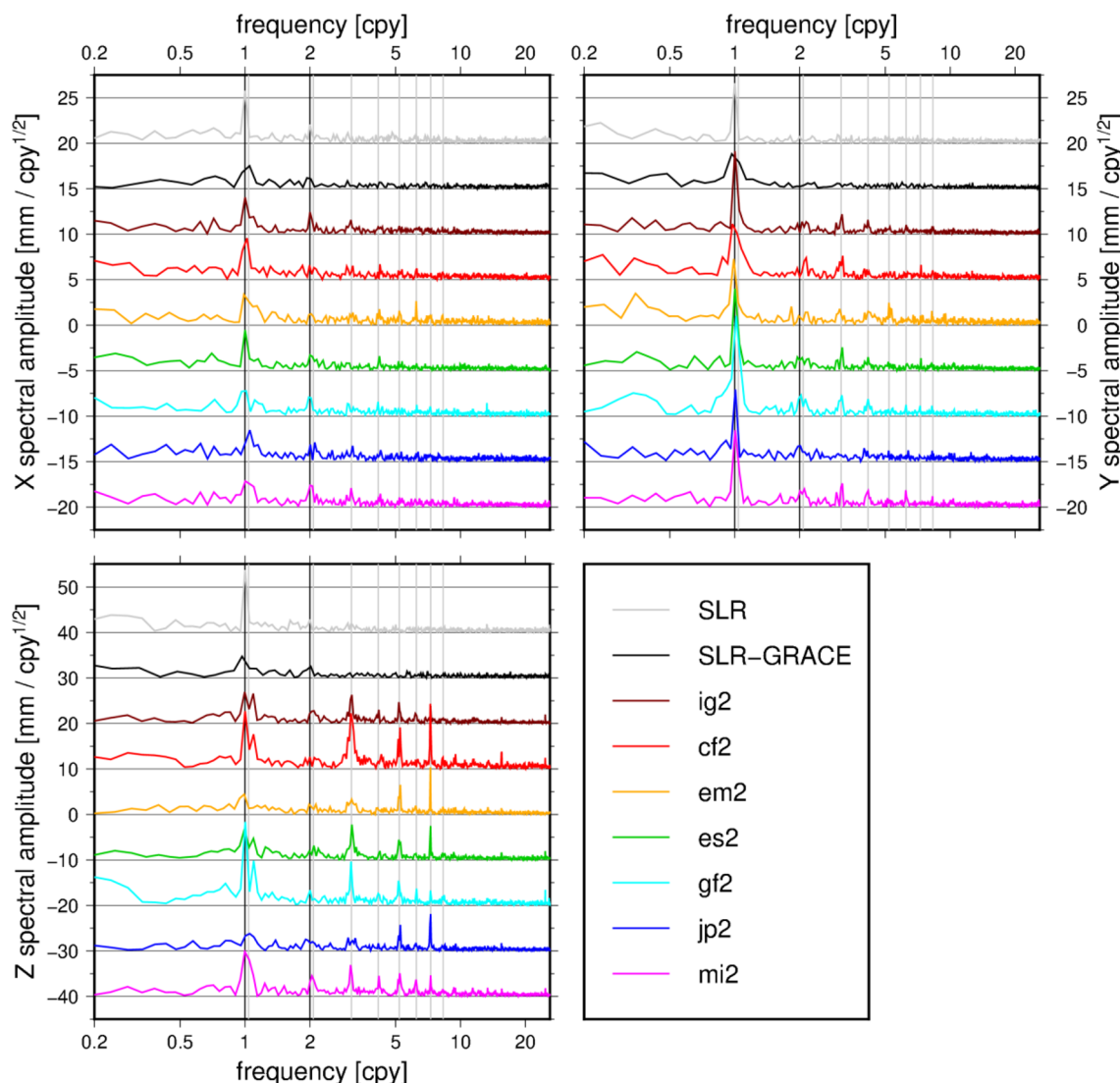


Fig. 2 Square root of the geocenter time series PSDs. Offsets of 5, 5 and 10 mm/ $\sqrt{\text{cpy}}$ have been added for clarity in the X , Y and Z directions. The black vertical lines indicate harmonics of the solar year, while the gray vertical lines indicate harmonics of the GPS draconitic year

Linear trends

The linear trends, i.e., offsets at epoch 2010.0 and rates, estimated for each geocenter time series are provided in Table 4 and represent long-term drifts with respect to the ITRF2014 origin. The offsets and rates of the (uncorrected) SLR time series are smaller than 1 mm and 0.1 mm/yr, and insignificant. This is expected since the SLR solutions were used to define the ITRF2014 origin. More interestingly, the uncertainties of those offsets and rates can be interpreted as uncertainties of the ITRF2014 origin. The rate uncertainties we obtained for the SLR time series are of ± 0.03 , ± 0.12 and ± 0.26 mm/yr in the X , Y and Z directions. In the Y and Z directions, they are comparable to the results of ± 0.17 and ± 0.33 mm/yr obtained by Riddell et al. (2017)

with wh + pl noise models. In the X direction, however, our rate uncertainty is considerably smaller, being based on a wh + AR(1) noise model (less correlated at long time lags than power-law noise).

The offsets of the SLR-GRACE geocenter time series remain smaller than 1 mm, but their trends reach 0.3 mm/yr in the Y and Z directions. Although these numbers are hardly statistically significant, they nevertheless indicate that mitigating the network effect via trend-free loading corrections can have a non-negligible impact on SLR-derived geocenter trends.

The offsets of the GNSS-derived geocenter time series are within ± 3 mm and hardly significant in the X and Y directions. In the Z direction, the estimated offsets are smaller than the value of 7 mm obtained by Rebischung et al. (2016)

Table 2 BIC values obtained from the adjustment of different noise models to the considered geocenter time series

	wh BIC	wh + pl BIC	wh + fl BIC	wh + GGM BIC	wh + AR(1) BIC
<i>X</i>					
SLR	5563.050	5361.626	5365.646	5356.872	5350.024
SLR–GRACE	437.018	419.856	417.412	422.197	416.489
ig2	43,008.049	39,762.029	39,796.759	39,769.215	40,273.067
cf2	47,945.926	46,550.720	46,568.393	46,557.098	46,609.899
em2	47,795.893	46,092.892	46,095.956	46,094.553	46,109.589
es2	43,787.224	42,145.282	42,163.672	42,153.315	42,240.623
gf2	47,256.099	45,490.068	45,509.001	45,498.200	45,577.204
jp2	48,551.041	46,385.851	46,413.368	46,393.023	46,512.578
mi2	46,617.721	43,468.621	43,516.210	43,475.608	43,683.313
<i>Y</i>					
SLR	5529.155	5006.261	5001.200	5011.664	5034.045
SLR–GRACE	347.965	333.499	331.446	335.821	331.613
ig2	43,424.864	38,934.712	38,923.545	38,938.263	39,027.909
cf2	48,578.349	46,284.980	46,274.374	46,287.061	46,308.483
em2	49,465.762	46,559.551	46,559.855	46,567.653	46,661.897
es2	44,289.797	42,280.800	42,272.970	42,276.441	42,291.636
gf2	47,666.472	45,173.504	45,162.019	45,171.151	45,193.971
jp2	47,829.150	45,578.746	45,570.703	45,575.824	45,654.266
mi2	46,890.925	42,902.055	42,898.056	42,907.312	43,011.105
<i>Z</i>					
SLR	6997.252	6619.560	6611.743	6621.040	6615.892
SLR–GRACE	533.013	528.779	527.224	532.199	527.798
ig2	50,381.600	43,699.748	43,685.273	43,675.175	43,526.217
cf2	61,738.634	56,813.591	56,799.221	56,554.584	56,529.958
em2	53,455.451	48,711.096	48,696.938	48,522.122	48,500.519
es2	51,353.879	46,823.246	46,809.479	46,715.791	46,707.137
gf2	58,461.002	53,903.658	53,890.172	53,867.066	53,883.092
jp2	53,110.273	49,191.736	49,178.304	49,023.688	49,021.128
mi2	54,160.257	48,160.170	48,145.635	47,925.403	47,921.018

The minimal BIC value for each time series is indicated in bold

from the comparison of the ig2 solutions with the IGB08 reference frame, mostly because of the 2.4 mm Z-translation between the origins of ITRF2008 and ITRF2014. A significant offset of about 4 mm on average yet remains between the average position of CM sensed by GNSS and the ITRF2014 origin. This offset could originate from errors in either GNSS geocenter estimates, SLR geocenter estimates, or in the local ties used to tie both technique networks in the ITRF2014 computation. There is, however, no way to know which error source predominates from the comparisons presented here.

The uncertainties of the rates of GNSS geocenter time series are about ± 0.1 , ± 0.2 and ± 0.1 mm/yr in the *X*, *Y* and *Z* components when realistic noise models are adopted, whereas they would be about ± 0.01 mm/yr only with a pure white noise model. In the *Y* and *Z* directions, the rates of the different GNSS geocenter time series are mostly negative

and seem to indicate respective trends of about -0.2 mm/yr and -0.1 mm/yr on average between GNSS geocenter estimates and the ITRF2014 origin, although these trends appear hardly significant. In the *X* direction, however, a significant trend of about 0.3 mm/yr on average can be observed, but we cannot say whether this disagreement is predominantly due to errors in GNSS geocenter estimates or in the SLR-based ITRF2014 origin.

Apparent annual variations

Before discussing the amplitudes and phases of the annual signals contained in the different geocenter time series, we deem it instructive to examine their apparent annual variations visually. Figure 4 thus shows the low-pass filtered series obtained with a Vondrák filter (Vondrák 1969, 1977) with 1.25 cpy cutoff frequency, i.e., the annual and

Table 3 Preferred noise models for the considered geocenter time series. The WRMS values are those of the residual geocenter time series, after the adjusted trends and periodic signals have been removed

	X			Y			Z					
	Preferred noise model	Spectral index	φ	WRMS (mm)	Preferred noise model	Spectral index	φ	WRMS (mm)	Preferred noise model	Spectral index	φ	WRMS (mm)
SLR	wh + AR(1)	—	0.74	2.81	wh + fl	—1	—2.81	wh + fl	—1	—1	—	5.17
SLR–GRACE	wh + AR(1)	—	0.80	2.44	wh + fl	—1	—2.36	wh + fl	—1	—1	—	4.59
ig2	wh + pl	—0.74	—	3.50	wh + fl	—1	—3.36	wh + AR(1)	—	—	0.93	5.36
cf2	wh + pl	—0.68	—	4.50	wh + fl	—1	—4.72	wh + AR(1)	—	—	0.93	10.37
em2	wh + pl	—0.79	—	5.48	wh + pl	—0.83	—6.24	wh + AR(1)	—	—	0.95	8.28
es2	wh + pl	—0.68	—	4.41	wh + fl	—1	—4.56	wh + AR(1)	—	—	0.93	7.22
gf2	wh + pl	—0.68	—	4.54	wh + fl	—1	—4.64	wh + GGM	—1.40	—	0.98	9.05
jp2	wh + pl	—0.67	—	5.16	wh + fl	—1	—4.83	wh + AR(1)	—	—	0.92	6.89
mi2	wh + pl	—0.74	—	4.44	wh + fl	—1	—4.33	wh + AR(1)	—	—	0.92	6.85

interannual variations of the series, plus the 1.04 cpy (fundamental draconitic frequency) variations of the GNSS series.

In the X direction, after about 2002, the apparent annual variations in GNSS and SLR series appear roughly in phase, and their low-frequency variations are generally in good agreement (compare for instance the ig2 series with the SLR series). In the Y direction, the apparent annual variations in GNSS and SLR series are also roughly in phase, over the whole period, although their amplitudes generally appear larger in GNSS series than in SLR series. In the Z direction, finally, the apparent annual variations in GNSS series appear alternatively in phase and out of phase with SLR, depending on the AC and time period considered, and show clear amplitude variations with time. As proposed by Rebischung et al. (2016), this behavior could be the result of alternatively constructive and destructive interferences between annual and draconitic variations, which is an explanation consistent with the fact that the Z component of GNSS geocenter estimates is more affected by draconitic errors than the X and Y components (see Fig. 2).

Note that this interference pattern varies among the different ACs. After 2006, in particular, the apparent annual variations in the Z component of the cf2, gf2 and the mi2 series are mostly out of phase with SLR, while the annual variations in the es2 series stay approximately in phase with SLR. Finally, the em2 and jp2 series show little trace of annual variations until about 2011, after which their apparent annual variations are also roughly in phase with SLR. These disparities between the apparent annual variations in the Z component of the IGS AC geocenter time series will be further discussed in the next section.

Annual signals

The amplitudes and phases of the annual sine waves estimated from each geocenter time series are shown in Figs. 5 and 6 and correspond to different estimates of annual geocenter motion. For the GNSS time series, these annual signals were estimated simultaneously with draconitic signals. This should, in principle, ensure that the estimated annual signals represent the annual variations in the series only, not a combination of their annual and draconitic variations. However, given the limited lengths of the series and the fact that both their annual and draconitic variations may not be stationary with time, the separation made between them may not be fully reliable.

In the X direction, the annual amplitudes in the GNSS time series are on average significantly smaller than the annual amplitude in the (uncorrected) SLR time series. However, the mitigation of network effect via loading corrections has a substantial impact on the amplitude of SLR-derived annual geocenter motion and brings the annual amplitude in the SLR–GRACE geocenter time series closer

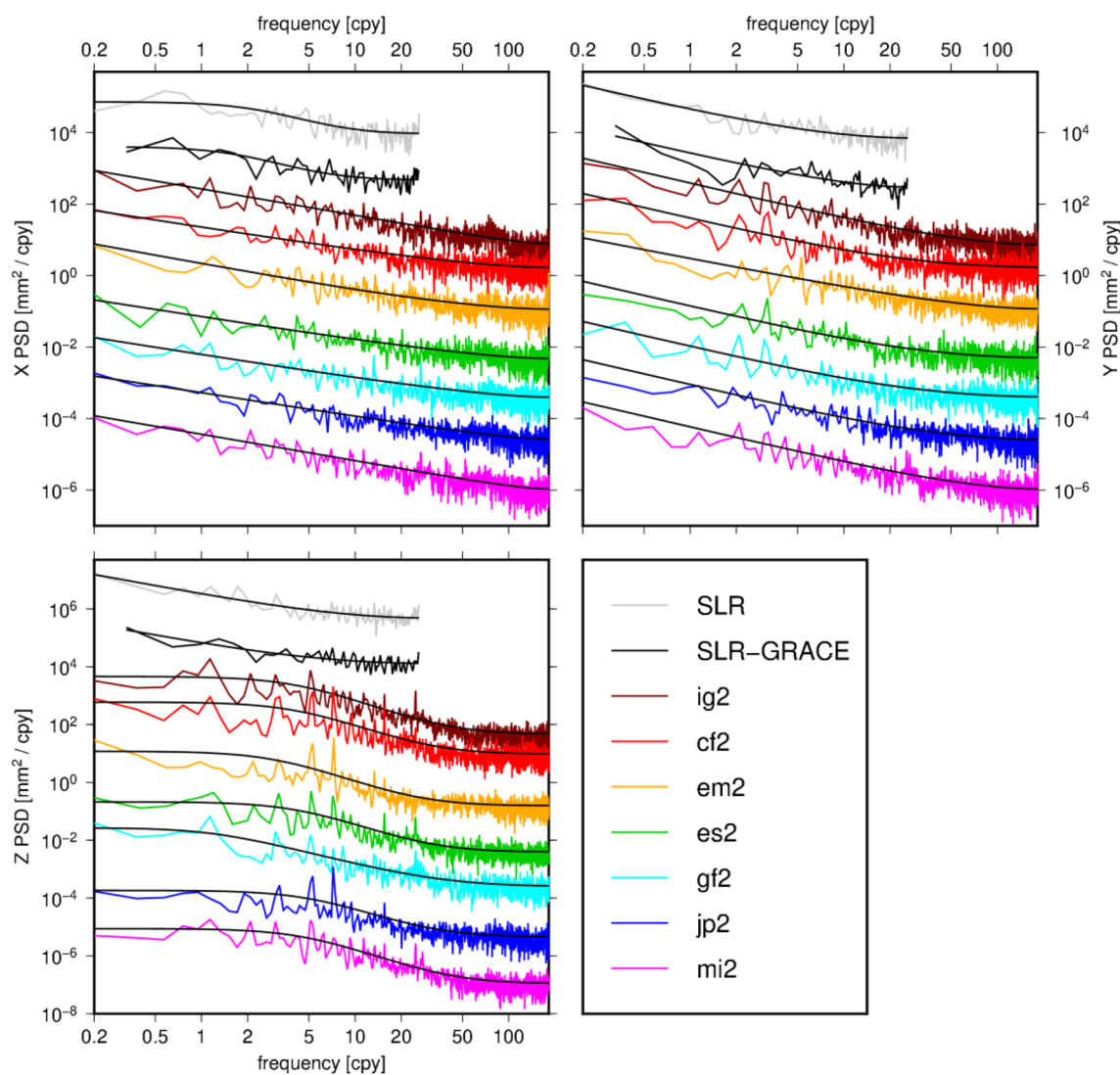


Fig. 3 PSDs of residual geocenter time series (with adjusted trends and periodic signals removed) and of the preferred noise models. Offsets have been added for clarity

Table 4 Estimated offsets (at epoch 2010.0) and rates of the considered geocenter time series

	<i>X</i>		<i>Y</i>		<i>Z</i>	
	Offset (mm)	Rate (mm/yr)	Offset (mm)	Rate (mm/yr)	Offset (mm)	Rate (mm/yr)
SLR	-0.06 ± 0.25	-0.02 ± 0.03	-0.31 ± 2.38	-0.01 ± 0.12	0.50 ± 5.12	-0.07 ± 0.26
SLR-GRACE	-0.12 ± 0.23	-0.12 ± 0.06	-0.14 ± 2.30	0.28 ± 0.20	0.29 ± 3.88	0.31 ± 0.34
ig2	0.77 ± 1.36	0.35 ± 0.09	-1.17 ± 2.91	-0.24 ± 0.18	4.16 ± 0.46	-0.07 ± 0.06
cf2	2.38 ± 1.23	0.23 ± 0.09	0.76 ± 3.61	-0.25 ± 0.22	2.28 ± 0.92	-0.05 ± 0.11
em2	0.23 ± 2.18	0.18 ± 0.14	-1.76 ± 3.11	0.09 ± 0.28	2.92 ± 0.71	-0.13 ± 0.09
es2	1.40 ± 1.04	0.19 ± 0.08	-0.63 ± 3.20	-0.02 ± 0.20	4.82 ± 0.52	-0.21 ± 0.07
gf2	2.22 ± 1.22	0.14 ± 0.09	-2.58 ± 3.40	-0.15 ± 0.20	3.84 ± 1.01	0.23 ± 0.12
jp2	-1.33 ± 1.32	0.30 ± 0.10	1.25 ± 3.84	-0.32 ± 0.23	5.26 ± 0.44	-0.24 ± 0.06
mi2	1.00 ± 1.70	0.47 ± 0.12	-2.75 ± 3.82	-0.35 ± 0.23	3.53 ± 0.52	-0.10 ± 0.07

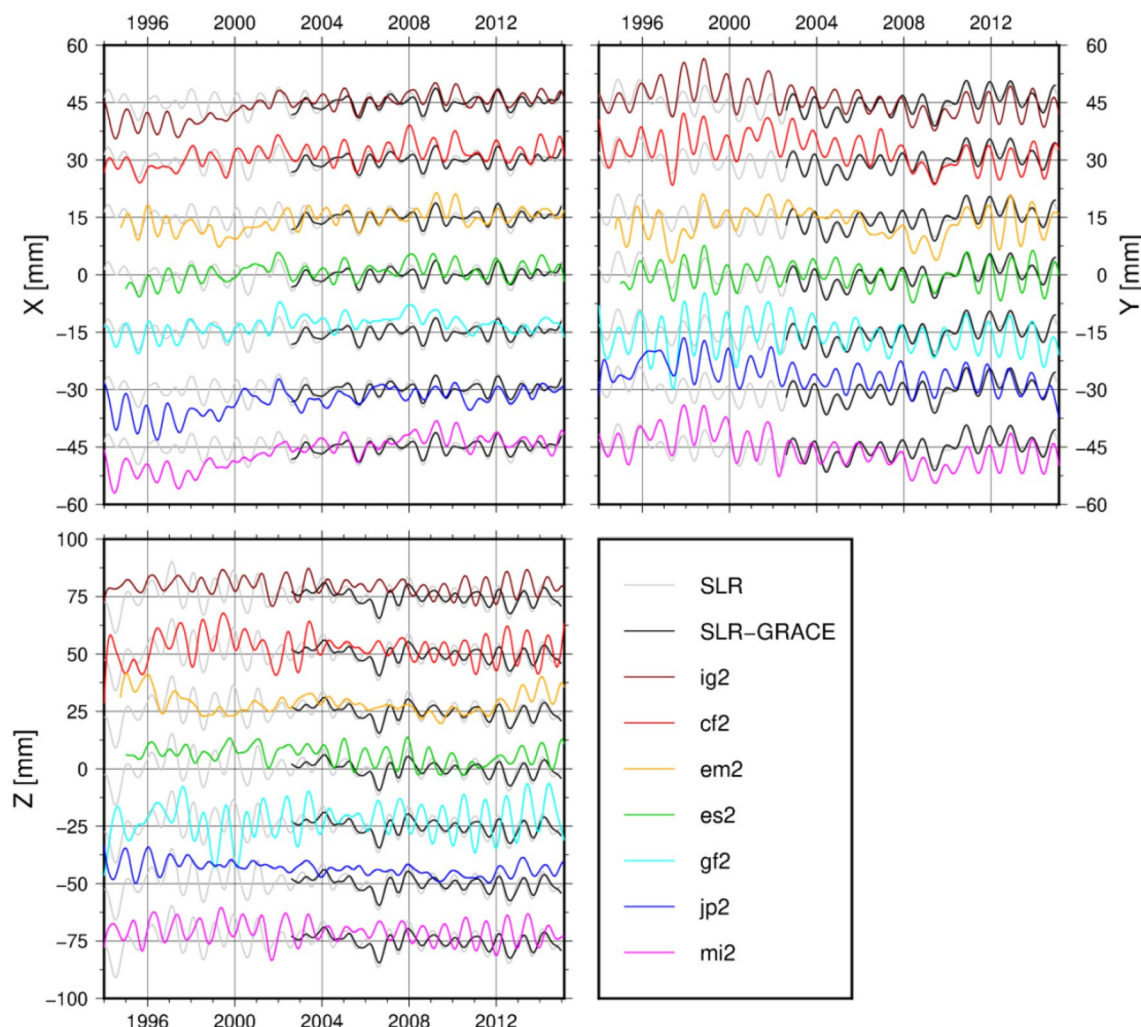


Fig. 4 Low-frequency variations of the considered geocenter time series, obtained with a Vondrák filter with 1.25 cpy cutoff frequency. The GNSS series are shown with different colors and offset from each

to those estimated from GNSS time series. A significant phase shift of the order of 30°–40° yet remains between the annual signals estimated from SLR and GNSS time series.

In the Y direction, the phases of the SLR and GNSS annual signals are in better agreement and differ by about 10° only on average. However, the amplitudes of the GNSS annual signals are notably larger (by about 1 mm on average) than those from both the SLR and SLR-GRACE time series. Despite those significant differences, which could be due to errors in either GNSS or SLR geocenter estimates, the annual signals estimated from SLR and GNSS geocenter time series are nevertheless in relatively good agreement in both the X and Y directions.

The situation is different in the Z direction, however, where there are large amplitude and phase differences between the SLR and GNSS annual signals, but also between the annual signals from the different GNSS series.

other. The SLR and SLR-GRACE time series are shown in gray and black, respectively, on top of each GNSS series to facilitate comparison

The annual signals derived from individual IGS AC time series can interestingly be grouped into two categories. Those estimated from the cf2, gf2 and mi2 time series have much larger amplitudes and phase shifts of more than 100° with respect to the annual signal from the SLR-GRACE time series. On the other hand, those estimated from the em2, es2 and jp2 time series show a much better agreement in amplitude and smaller phase differences with respect to the annual signal from the SLR-GRACE time series.

GNSS geocenter estimates, particularly in the Z direction, are known to be sensitive to orbit modeling errors and to the modeling of solar radiation pressure in particular (Dong et al. 2003; Rodriguez-Solano et al. 2012; Meindl et al. 2013). To generate their repro2 solutions, the CODE, GFZ and MIT ACs (i.e., those whose annual geocenter signals show large differences with SLR in Z) used purely empirical approaches to account for solar radiation pressure, by

Fig. 5 Amplitudes of the annual signals estimated from the considered geocenter time series

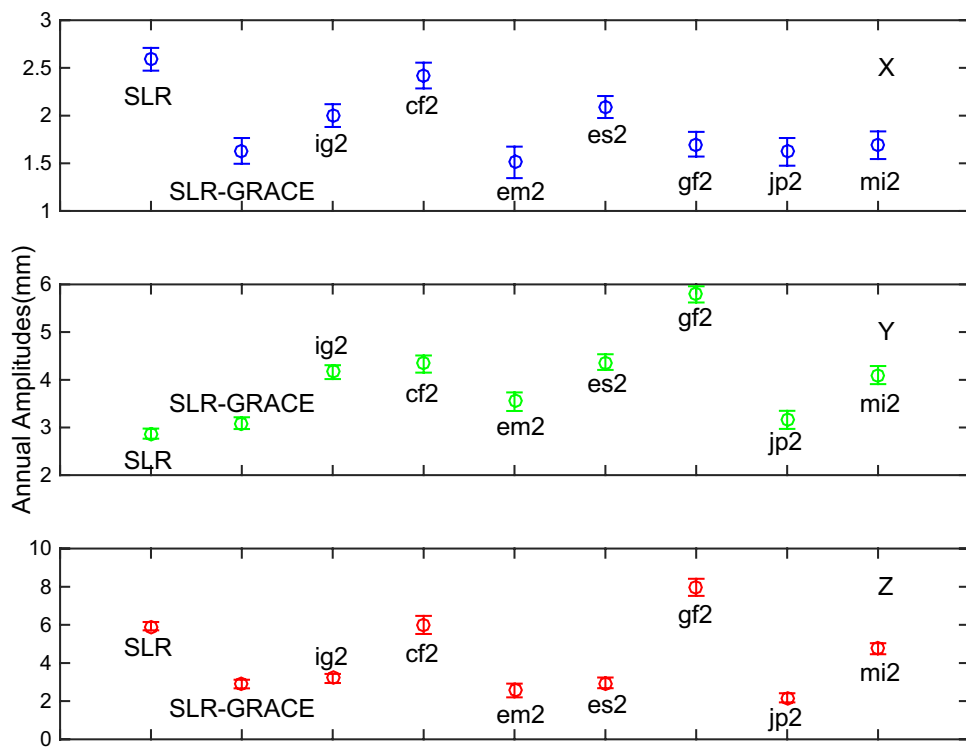
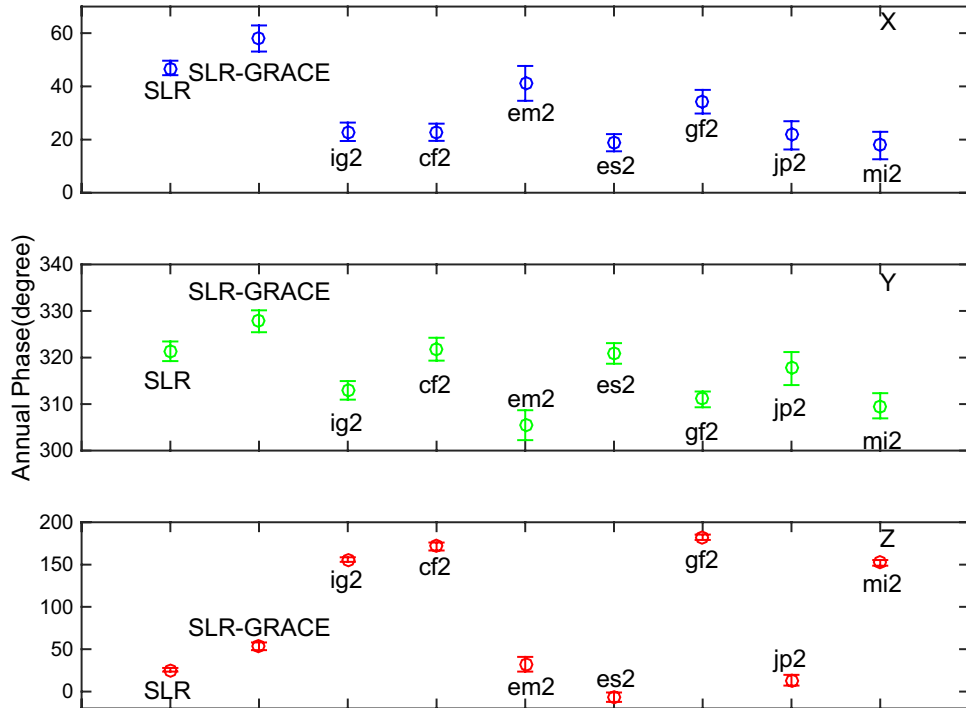


Fig. 6 Phases of the annual signals estimated from the considered geocenter time series



estimating different subsets of extended CODE orbit model (ECOM; Beutler et al. 1994) parameters, on top of which CODE and GFZ also estimated pseudo-stochastic velocity changes at noon for all satellites. The ESA AC, whose annual Z geocenter signal is closer to SLR, also estimated empirical ECOM parameters as well as constrained constant

and once-per-revolution along-track accelerations, but additionally incorporated a priori box-wing solar radiation pressure models (Springer et al. 2014). Finally, EMR and JPL also used a priori solar radiation pressure models (GSPM13; Sibois et al. 2014) on top of which they estimated stochastic empirical accelerations. It would, therefore, seem that the

use of a priori solar radiation pressure models has a clear positive impact on GNSS-derived annual geocenter motion in Z, bringing it closer to SLR-derived estimates.

Residual variations

Figure 7 shows the residual geocenter time series, after the adjusted trends and periodic signals have been removed. Table 5 provides the correlation coefficients between the SLR residual time series and weekly averages of the GNSS residual time series, computed over the period of the SLR–GRACE time series. The correlation coefficients are systematically positive and mostly range from 0.3 to 0.4 in the X and Y directions. This could indicate that part of the residual variations might correspond to real, aperiodic geocenter motion commonly observed by SLR and GNSS and not only measurement errors.

An apparent offset is in particular visible around epoch 2010.0 in the Y component of both SLR series and of some GNSS series. This offset had been noticed by Altamimi et al. (2016) in their SLR geocenter time series. Riddell et al. (2017) analyzed the same SLR series and tried to estimate this offset but found it to be insignificant and therefore likely “simply characteristic of power-law time-correlated noise.” We similarly tried to estimate this offset in both our SLR and GNSS time series (Table 6) and reached the same conclusion. Yet, the fact that this offset appears not only in SLR but also in GNSS geocenter time series suggests that it could stem from real geocenter motion rather than SLR errors.

The correlation coefficients between SLR and GNSS residual geocenter time series are smaller in the Z direction than in the X and Y directions, possibly due to larger errors in GNSS Z geocenter estimates. The correlation coefficient between the SLR–GRACE and es2 time series nevertheless

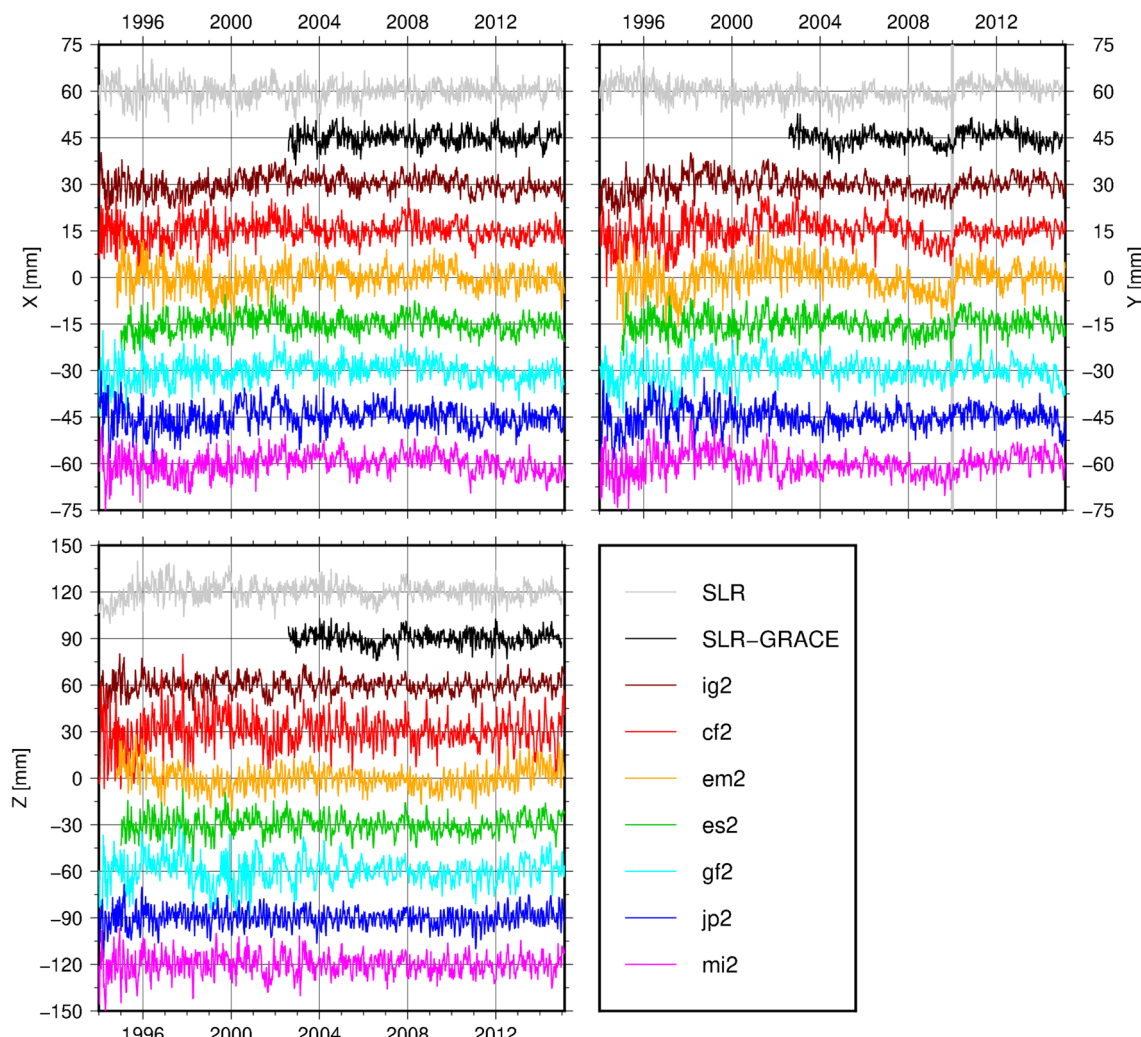


Fig. 7 Residual geocenter time series (with adjusted trends and periodic signals removed). Offsets by 15, 15 and 30 mm have been added for clarity. The vertical gray line in the second panel indicates epoch 2010.0

Table 5 Correlation coefficients between SLR and GNSS residual geocenter time series

	ig2	cf2	em2	es2	gf2	jp2	mi2
<i>X</i>							
SLR	0.34	0.32	0.27	0.31	0.30	0.32	0.25
SLR–GRACE	0.38	0.33	0.29	0.31	0.32	0.36	0.29
<i>Y</i>							
SLR	0.40	0.24	0.27	0.26	0.21	0.37	0.42
SLR–GRACE	0.41	0.36	0.38	0.30	0.36	0.32	0.31
<i>Z</i>							
SLR	0.11	0.14	0.15	0.20	0.08	0.12	0.04
SLR–GRACE	0.12	0.15	0.18	0.23	0.06	0.15	0.06

Table 6 Offsets estimated at epoch 2010.0 from the residual geocenter time series in the *Y* direction (mm)

ig2	1.49 ± 1.44	cf2	2.34 ± 2.06	em2	2.14 ± 2.36
gf2	0.42 ± 1.90	jp2	1.53 ± 1.98	mi2	2.26 ± 1.94
es2	1.78 ± 1.76	SLR	2.34 ± 2.23	SLR–GRACE	1.66 ± 1.14

reaches 0.23. This might be an indication that ESA's solar radiation pressure modeling allows to better sense not only annual but also aperiodic geocenter motion in *Z*.

Summary

Geocenter motion time series derived from the IGS repro2 combined solutions and six individual AC contributions have been analyzed and compared to two SLR geocenter time series—the first one obtained by direct comparison of the weekly SLR input solutions to ITRF2014, the second one obtained from the same weekly SLR solutions corrected from GRACE-derived loading displacements. All the time series have been shown to exhibit time-correlated noise, best modeled by either white plus power-law, white plus AR(1), or white plus GGM noise models, depending on the technique and the component. Linear trends and periodic signals (annual and semi-annual for SLR; additional draconitic signals for GNSS) have been fitted to the different geocenter time series, accounting for the presence of correlated noise in the series.

The estimated trends represent long-term drifts with respect to the ITRF2014 origin. Their analysis shows that: (1) The mitigation of the network effect via trend-free loading corrections has a non-negligible impact on SLR-derived geocenter trends (up to about 0.3 mm/yr in the *Y* and *Z* components). (2) The differences between SLR-derived and GNSS-derived geocenter trends are generally insignificant, except an offset of about 4 mm in the *Z* component and a rate of about 0.3 mm/yr in the *X* component. Our comparisons do, however, not allow to determine whether these

inconsistencies stem from errors in SLR geocenter estimates, in GNSS geocenter estimates or in the inter-technique ties used in the ITRF2014 computation.

The estimated annual signals provide different estimates of annual geocenter motion. As for the long-term trends, it can be observed that the mitigation of the network effect via loading corrections has a non-negligible impact on SLR-derived annual geocenter motion (amplitude reduced by about 1 mm in *X*; about 3 mm in *Z*). In the *X* and *Y* directions, the annual signals in the GNSS time series are in relatively good agreement with the annual signal from the SLR–GRACE time series. In the *Z* direction, the annual signals in GNSS time series show large disparities but can be grouped into two categories. Those derived from AC solutions in which solar radiation pressure is accounted for purely empirically (cf2, gf2, mi2) show large disagreements in amplitude and phase with the annual signal from the SLR–GRACE time series. On the other hand, those derived from AC solutions in which a priori solar radiation pressure models have been incorporated (em2, es2, jp2) show better agreement with the annual signal from the SLR–GRACE time series. This suggests that the use of a priori solar radiation pressure models has a clear positive impact on the *Z* component of GNSS-derived annual geocenter motion.

We finally compared the residual GNSS and SLR geocenter time series, with their adjusted trends and periodic signals removed. The correlation coefficients between GNSS and SLR residual time series are systematically positive, around 0.3–0.4 in the *X* and *Y* directions. This could indicate that part of the residual variations in both GNSS and SLR geocenter time series might reflect real, aperiodic geocenter motion. The correlation coefficients in the *Z* direction are smaller, but the correlation between the SLR–GRACE and es2 time series nevertheless reaches 0.23. This might be an indication that ESA's solar radiation pressure modeling allows to better sense not only annual but also aperiodic geocenter motion in the *Z* component.

In conclusion, it appears that despite orbit modeling and collinearity issues, GNSS geocenter estimates obtained with

the network shift approach are in reasonable agreement with SLR in the *X* and *Y* directions. In the *Z* direction, it seems that the a priori modeling of solar radiation pressure has a considerable impact on GNSS geocenter estimates, so that progress in this field may eventually lead to a reliable determination of geocenter motion with GNSS and the network shift approach.

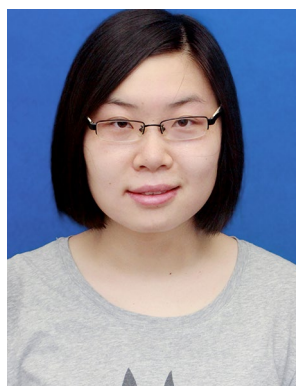
Acknowledgements This study is supported by the National Science Fund for Distinguished Young Scholars (No. 41525014) and the National Key R&D Program of China (No. 2018YFC15036). The Chinese Scholarship Council (CSC) has provided the first author a scholarship which allowed her to visit IGN in France for one year, starting in December 2017. We acknowledge the efforts made by the IGS, ILRS and their individual Analysis Centers to provide the reprocessed solutions on which this study is based. This is IPGP contribution number 4084.

References

- Altamimi Z, Rebischung P, Métivier L, Collilieux X (2016) ITRF2014: A new release of the international terrestrial reference frame modeling non-linear station motions. *J Geophys Res Solid Earth* 121:6109–6131. <https://doi.org/10.1002/2016JB013098>
- Amiri-Simkooei AR (2007) Least-squares variance component estimation: theory and GPS applications. Ph.D. thesis, Delft University of Technology
- Amiri-Simkooei AR (2009) Noise in multivariate GPS position time series. *J Geod* 83(2):175–187. <https://doi.org/10.1007/s00190-008-0251-8>
- Amiri-Simkooei AR, Mohammadloo TH, Argus DF (2017) Multivariate analysis of GPS position time series of JPL second reprocessing campaign. *J Geod* 91(6):685–704. <https://doi.org/10.1007/s00190-016-0991-9>
- Beutler G, Brockmann E, Gurtner W, Hugentobler U, Mervart L, Rothacher M, Verdun A (1994) Extended orbit modeling techniques at the CODE Processing Center of the International GPS Service for geodynamics (IGS): theory and initial results. *Manuscr Geod* 19(6):367–386
- Blewitt G, Heflin MB, Webb FH, Lindqwister UJ, Malla RP (1992) Global coordinates with centimeter accuracy in the International Terrestrial Reference Frame Using GPS. *Geophys Res Lett* 19(9):853–856. <https://doi.org/10.1029/92GL00775>
- Blewitt G, Lavallée D, Clarke P, Nurutdinov K (2001) A new global mode of Earth deformation: seasonal cycle detected. *Science* 294(5550):2342–2345. <https://doi.org/10.1126/science.1065328>
- Blewitt G (2003) Self-consistency in reference frames, geocenter definition, and surface loading of the solid Earth. *J Geophys Res* 108(B2):2103. <https://doi.org/10.1029/2002JB002082>
- Blewitt G, Clarke P (2003) Inversion of Earth's changing shape to weigh sea level in static equilibrium with surface mass redistribution. *J Geophys Res.* <https://doi.org/10.1029/2002JB002290>
- Bos MS, Fernandes RMS, Williams SDP, Bastos L (2013) Fast error analysis of continuous GNSS observations with missing data. *J Geod* 87(4):351–360. <https://doi.org/10.1007/s00190-012-0605-0>
- Bos M, Fernandes R (2019) Hector user manual version 1.7.2. https://segal.ubi.pt/hector/manual_1.7.2.pdf
- Chanard K, Fleitout L, Calais E, Rebischung P, Avouac JP (2018) Toward a global horizontal and vertical elastic load deformation model derived from GRACE and GNSS station position time series. *J Geophys Res* 123(4):3225–3237. <https://doi.org/10.1002/2017JB015245>
- Collilieux X, Altamimi Z, Ray J, van Dam T, Wu X (2009) Effect of the satellite laser ranging network distribution on geocenter motion estimation. *J Geophys Res* 114:B04402. <https://doi.org/10.1029/2008JB005727>
- Collilieux X, van Dam T, Ray J, Coulot D, Métivier L, Altamimi Z (2012) Strategies to mitigate aliasing of loading signals while estimating GPS frame parameters. *J Geod* 86(1):1–14. <https://doi.org/10.1007/s00190-011-0487-6>
- Deng Z, Gendt G, Schöne T, Nischan T, Fritsche M (2014) IGS 2nd reprocessing at GFZ. *IGS workshop 2014*, Pasadena, USA, 23–27 June
- Desai SD, Bertiger W, Garcia-Fernandez M, Haines B, Murphy D, Selle C, Sibois A, Sibthorpe A, Weiss JP (2014) Status and Plans at the JPL IGS Analysis Center. *IGS workshop 2014*, Pasadena, USA, 23–27 June
- Donahue B, Ghoddousi-Fard R, Mireault Y (2014) Current status and future plans at the Natural Resources Canada (NRCan) Analysis Centre. *IGS workshop 2014*, Pasadena, USA, 23–27 June
- Dong D, Dickey JO, Chao Y, Cheng MK (1997) Geocenter variations caused by atmosphere, ocean and surface ground water. *Geophys Res Lett* 24(15):1867–1870. <https://doi.org/10.1029/97GL01849>
- Dong D, Yunck T, Heflin M (2003) Origin of the International Terrestrial Reference Frame. *J Geophys Res* 108(B4):2200. <https://doi.org/10.1029/2002JB002035>
- Johnston G, Riddell A, Hausler G (2017) In: Teunissen PJ, Montenbruck O (eds) Springer handbook of global navigation satellite systems. Springer handbooks. Springer, Cham. <https://doi.org/10.1007/978-3-319-42928-1>
- Kang Z, Tapley B, Chen J, Ries J, Bettadpur S (2019) Geocenter motion time series derived from GRACE GPS and LAGEOS observations. *J Geod* 93(10):1931–1942. <https://doi.org/10.1007/s00190-019-01292-4>
- Lavallee DA, van Dam T, Blewitt G, Clarke PJ (2006) Geocenter motions from GPS: a unified observation model. *J Geophys Res* 111:B05405. <https://doi.org/10.1029/2005JB003784>
- Lemoine J-M, Bruinsma S, Gégoût P, Biancale R, Bourgogne S (2013) Release 3 of the GRACE gravity solutions from CNES/GRGS. *EGU General Assembly 2013*, Vienna, Austria, 7–12 Apr
- Mao A, Harrison CGA, Dixon TH (1999) Noise in GPS coordinate time series. *J Geophys Res* 104(B2):2797–2816. <https://doi.org/10.1029/1998JB900033>
- Meindl M, Beutler G, Thaller D, Dach R, Jäggi A (2013) Geocenter coordinates estimated from GNSS data as viewed by perturbation theory. *Adv Space Res* 51(7):1047–1064. <https://doi.org/10.1016/j.asr.2012.10.026>
- Pearlman MR, Degnan JJ, Bosworth JM (2002) The international laser ranging service. *Adv Space Res* 30(2):135–143. [https://doi.org/10.1016/S0273-1177\(02\)00277-6](https://doi.org/10.1016/S0273-1177(02)00277-6)
- Petit G, Luzum B (2010) IERS Technical Note 36
- Ray J, (1999) IERS Analysis campaign to investigate motions of the geocenter. IERS technical note 25
- Ray J, Altamimi Z, Collilieux X, van Dam T (2008) Anomalous harmonics in the spectra of GPS position estimates. *GPS Solut* 12(1):55–64. <https://doi.org/10.1007/s10291-007-0067-7>
- Rebischung P, Altamimi Z, Springer T (2014) A collinearity diagnosis of the GNSS geocenter determination. *J Geod* 88(1):65–85. <https://doi.org/10.1007/s00190-013-0669-5>
- Rebischung P, Altamimi Z, Ray J, Garayt B (2016) The IGS contribution to ITRF2014. *J Geod* 90(7):611–630. <https://doi.org/10.1007/s00190-016-0897-6>

- Rebisching P, Schmid R (2016) IGS14/igs14.atx: a new framework for the IGS products. AGU Fall Meeting 2016, San Francisco, USA, 12–16 Dec
- Riddell AR, King AM, Watson CS, Sun Y, Riva REM, Rietbroek R (2017) Uncertainty in geocenter estimates in the context of ITRF2014. *J Geophys Res Solid Earth* 122(5):4020–4032. <https://doi.org/10.1002/2016JB013698>
- Ries JC (2016) Reconciling estimates of annual geocenter motion from space geodesy. In: Proceedings of the 20th international workshop on laser ranging, Potsdam, Germany, 10–14 Oct 2016. https://cds.nasa.gov/lw20/docs/2016/papers/14-Ries_paper.pdf
- Rodriguez-Solano CJ, Hugentobler U, Steigenberger P (2012) Adjustable box-wing model for solar radiation pressure impacting GPS satellites. *Adv Space Res* 49(7):1113–1128. <https://doi.org/10.1016/j.asr.2012.01.016>
- Santamaría-Gómez A, Bouin MN, Collilieux X, Wöppelmann G (2011) Correlated errors in GPS position time series: Implications for velocity estimates. *J Geophys Res Solid Earth* 116(B1):B01405. <https://doi.org/10.1029/2010JB007701>
- Scargle J (1982) Studies in astronomical time series analysis. II-statistical aspects of spectral analysis of unevenly spaced data. *Astrophys J* 263:835–853. <https://doi.org/10.1086/160554>
- Schwarz G (1978) Estimating the dimension of a model. *Ann Stat* 6(2):461–464
- Sibois A, Selle C, Desai S, Sibthorpe A, Weiss J (2014) GSPM13: An updated empirical model for solar radiation pressure forces acting on GPS satellites. IGS workshop 2014, Pasadena, USA, 23–27 June
- Springer T, Flohrer C, Otten M, Enderle W (2014) ESA reprocessing: advances in GNSS analysis. IGS workshop 2014, Pasadena, USA, 23–27 June
- Steigenberger P, Lutz S, Dach R, Schaer S, Jäggi A (2014) CODE repro2 product series for the IGS. Astronomical Institute, University of Bern, Bern CHE. <https://doi.org/10.7892/boris.75680>
- Vondrák J (1969) A contribution to the problem of smoothing observational data. *Bull Astron Inst Czechoslov* 20(6):349–355
- Vondrák J (1977) Problem of smoothing observational data II. *Bull Astron Inst Czechoslov* 28(2):84–89
- Williams SDP, Bock Y, Fang P, Jamason P, Nikolaidis RM, Prawirodirdjo L, Miller M, Johnson DJ (2004) Error analysis of continuous GPS position time series. *J Geophys Res* 109:B03412. <https://doi.org/10.1029/2003JB002741>
- Wu X, Ray J, van Dam T (2012) Geocenter motion and its geodetic and geophysical implications. *J Geodyn* 58:44–61. <https://doi.org/10.1016/j.jog.2012.01.007>
- Zhang J, Bock Y, Johnson H, Fang P, Williams S, Genrich J, Wdowinski S, Behr J (1997) Southern California permanent GPS geodetic array: error analysis of daily position estimates and site velocities. *J Geophys Res Solid Earth* 102(B8):18035–18055. <https://doi.org/10.1029/97JB01380>
- Zhang X, Jin S (2014) Uncertainties and effects on geocenter motion estimates from global GPS observations. *Adv Sp Res* 54(1):59–71. <https://doi.org/10.1016/j.asr.2014.03.021>
- Zou R, Freymueller JT, Ding K, Yang S, Wang Q (2014) Evaluating seasonal loading models and their impact on global and regional reference frame alignment. *J Geophys Res Solid Earth* 119:1337–1358. <https://doi.org/10.1002/2013JB010186>

Publisher's Note Springer Nature remains neutral with regard to jurisdictional claims in published maps and institutional affiliations.



Yifang Ma works at Beijing Earthquake Agency. She received her Ph.D. degree in Geodesy and Engineering Surveying from Wuhan University in 2019. Her main interests are Global Navigation Satellite Systems and terrestrial reference frames.



Paul Rebischung works at the Geodesy Department of the Institut de Physique du Globe de Paris (IPGP) and at the Institut National de l'Information Géographique et Forestière (IGN), France. His research interests are terrestrial reference frames and Global Navigation Satellite Systems. He received his Ph.D. degree in Astronomy and Astrophysics from the Paris Observatory in 2014.



Zuheir Altamimi is head of the terrestrial reference systems research group of the Geodesy Department of IPGP-IGN, France. He is head of the International Terrestrial Reference System (ITRS) Product Center of the IERS. His principal research focus is the theory and realization of terrestrial reference systems. He received his Ph.D. from the Paris Observatory in 1990, and his habilitation (professorial thesis) from the University of Paris VI in 2006.



Weiping Jiang is currently a professor at Wuhan University. He obtained his B.Sc., Master and Ph.D. degrees with distinction in Geodesy and Engineering Surveying at the School of Geodesy and Geomatics at Wuhan University in 1995, 1997 and 2001. His main research interests include GNSS data processing of large-scale networks, GNSS coordinate time series analysis, satellite altimetry and geodynamics research.